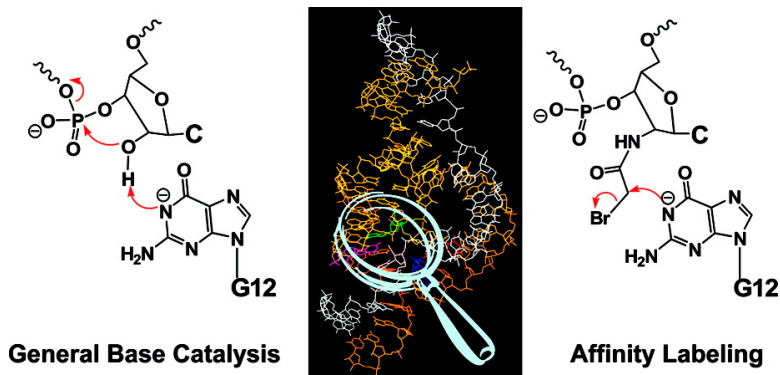


## Probing General Base Catalysis in the Hammerhead Ribozyme

Jason M. Thomas, and David M. Perrin

*J. Am. Chem. Soc.*, **2008**, 130 (46), 15467-15475 • DOI: 10.1021/ja804496z • Publication Date (Web): 25 October 2008

Downloaded from <http://pubs.acs.org> on February 8, 2009



### More About This Article

Additional resources and features associated with this article are available within the HTML version:

- Supporting Information
- Links to the 1 articles that cite this article, as of the time of this article download
- Access to high resolution figures
- Links to articles and content related to this article
- Copyright permission to reproduce figures and/or text from this article

[View the Full Text HTML](#)



**ACS Publications**  
 High quality. High impact.

## Probing General Base Catalysis in the Hammerhead Ribozyme

Jason M. Thomas and David M. Perrin\*

Department of Chemistry, University of British Columbia, 2036 Main Mall, Vancouver, British Columbia, Canada, V6T 1Z1

Received June 12, 2008; E-mail: dperrin@chem.ubc.ca

**Abstract:** Recent structural and computational studies have shed new light on the catalytic mechanism and active site structure of the RNA cleaving hammerhead ribozyme. Consequently, specific ribozyme functional groups have been hypothesized to be directly involved in general/acid base catalysis. In order to test this hypothesis, we have developed an affinity label to identify the functional general base in the *S. mansoni* hammerhead ribozyme. The ribozyme was reacted with a substrate analogue bearing a 2'-bromoacetamide group in place of the nucleophilic 2'-hydroxyl group which would normally be deprotonated by a general base. The electrophilic 2'-bromoacetamide group is poised to alkylate the general base, which is subsequently identified by footprinting analysis. Herein, we demonstrate alkylation of N1 of G12 in the hammerhead ribozyme in a pH and  $[Mg^{2+}]$  dependent manner that is consistent with the native cleavage reaction. These results provide substantial evidence that deprotonated N1 of G12 functions directly as a general base in the hammerhead ribozyme; moreover, our experiments provide evidence that the  $pK_a$  of G12 is perturbed downward in the context of the active site structure. We also observed other pH-independent alkylations, which do not appear to reflect the catalytic mechanism, but offer further insight into ribozyme conformation and structure.

### Introduction

The naturally occurring hammerhead ribozyme has been the subject of intense mechanistic and structural investigation for some 20 years. Despite a plethora of detailed biochemical and crystallographic data, the active site structure and mechanism has remained very obscure until recently.<sup>1,2</sup> Earlier studies focused on so-called "minimal" hammerhead constructs such as the HH16 (Figure 1A).<sup>3</sup> Divalent metal cations ( $M^{2+}$  generally,  $Mg^{2+}$  specifically) appeared to play an important role in hammerhead activity, and specific interactions with both ribozyme and substrate have been characterized.<sup>4–6</sup> These findings prompted speculation that the  $M^{2+}$  provided Lewis acid and/or general acid/base catalysis (in its hydrated forms).<sup>5,7,8</sup> However, because activity was observed in the presence of monovalent cations or exchange inert  $Co(NH_3)_6^{3+}$  alone,<sup>9–11</sup>

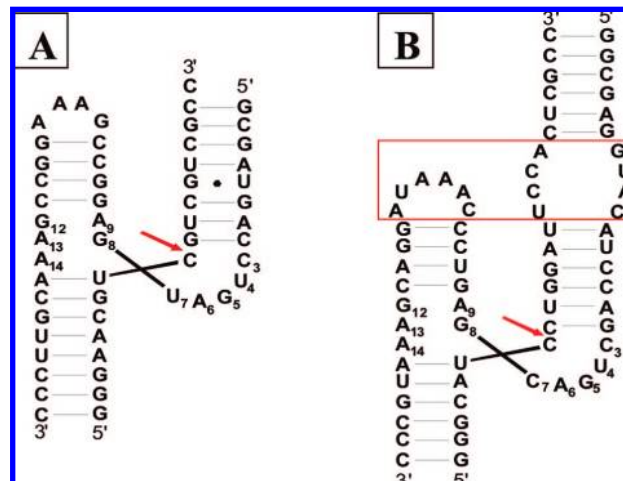


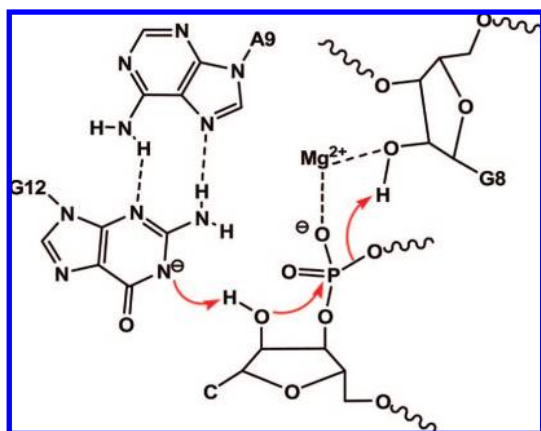
**Figure 1.** Secondary structures of the HH16 (minimal) and *S. mansoni* (extended) hammerhead ribozymes bound to their respective substrates. The substrate cleavage sites are indicated by the red arrows, and the nucleotides in the conserved catalytic core are numbered according to convention. The loops involved in the additional tertiary stabilization of the extended hammerhead are highlighted by the red box.

other mechanistic explanations, including direct nucleobase participation in catalysis, remained a possibility. Unfortunately, the crystal structures of minimal hammerhead ribozymes<sup>12–14</sup> provided little mechanistic insight and were contradicted by

- (1) Blount, K. F.; Uhlenbeck, O. C. *Annu. Rev. Biophys. Biomol. Struct.* **2005**, *34*, 415–440.
- (2) Nelson, J. A.; Uhlenbeck, O. C. *RNA* **2008**, *14*, 605–615.
- (3) Hertel, K. J.; Herschlag, D. J. A.; Uhlenbeck, O. C. *Biochemistry* **1994**, *33*, 3374–3385.
- (4) Peracchi, A.; Beigelman, L.; Scott, E. C.; Uhlenbeck, O. C.; Herschlag, D. *J. Biol. Chem.* **1997**, *272*, 26822–26826.
- (5) Cunningham, L. A.; Li, J.; Lu, Y. *J. Am. Chem. Soc.* **1998**, *120*, 4518–4519.
- (6) Wang, S.; Karbstein, K.; Peracchi, A.; Beigelman, L.; Herschlag, D. *Biochemistry* **1999**, *38*, 14363–14378.
- (7) Sawata, S.; Komiyama, M.; Taira, K. *J. Am. Chem. Soc.* **1995**, *117*, 2357–2358.
- (8) Pontius, B. W.; Lott, W. B.; von Hippel, P. H. *Proc. Natl. Acad. Sci.* **1997**, *94*, 2290–2294.
- (9) O'Rear, J. L.; Wang, S.; Feig, A. L.; Beigelman, L.; Uhlenbeck, O. C.; Herschlag, D. *RNA* **2001**, *7*, 537–545.
- (10) Murray, J. B.; Seyhan, A. A.; Walter, N. G.; Burke, J. M.; Scott, W. G. *Chem. Biol.* **1998**, *5*, 587–595.

- (11) Curtis, E. A.; Bartel, D. P. *RNA* **2001**, *7*, 546–552.
- (12) Scott, W. G.; Finch, J. T.; Klug, A. *Cell* **1995**, *81*, 991–1002.
- (13) Scott, W. G.; Murray, J. B.; Arnold, J. R.; Stoddard, B. L.; Klug, A. *Science* **1996**, *274*, 2065–2069.

**Scheme 1.** Possible Catalytic Mechanism Where G12 Acts As the General Base in Concert with the 2'-OH of G8 Acting As the General Acid



many biochemical studies.<sup>2</sup> In light of these contradictions, one could hypothesize that these crystal structures, while informative, represent an inactive conformation of the ribozyme/substrate complex: either a ground-state or an entirely inconsequential structure as has been observed in an attempt to crystallize the 10–23 DNAzyme.<sup>15</sup>

More recent studies have focused on so-called “extended” motifs, such as the *S. mansoni* hammerhead (Figure 1B), which include more of their natural occurring peripheral sequences. An additional tertiary interaction in these extended ribozymes appears to stabilize an active conformation, leading to more efficient catalysis and reduced divalent metal ion requirements relative to the minimal hammerheads.<sup>16,17</sup> Recent photocross-linking<sup>18,19</sup> and nucleobase  $pK_a$ -perturbation<sup>20</sup> experiments have suggested that two hammerhead nucleobases, G8 and G12, are proximal to the cleavage site in the active ribozyme conformation and may play direct roles in general acid/base catalysis. These results further contradicted the minimal hammerhead crystal structures, and foreshadowed the findings from the recent groundbreaking crystal structure obtained for an extended hammerhead.<sup>21</sup>

The extended hammerhead crystal structure appears to reconcile much of the previous biochemical data, suggesting that this structure reflects the catalytically competent conformation.<sup>2</sup> On the basis of the observed active site structure, a catalytic mechanism (Scheme 1) has been proposed in which G12 acts directly as a general base and the 2'-OH of G8 as a general acid.<sup>22–24</sup> The precise mechanistic role of metal cations

could not be resolved crystallographically. Recent computational studies support this proposed mechanism and suggest that a metal ion may stabilize negative charge on a nonbridging oxygen in the transition state, as well as coordinate the G8 2'-OH to lower its  $pK_a$  and facilitate acid catalysis.<sup>22,25,26</sup> Of note, Burke and co-workers have recently found that substitution of  $Cd^{2+}$  for  $Mg^{2+}$  leads to a drastic change in the pH-rate profile consistent with  $M^{2+}$ -mediated general acid catalysis.<sup>27</sup> No involvement of a  $M^{2+}$  in general base catalysis has been indicated, consistent with the hypothesis of direct nucleobase involvement.

The apparent congruence of the extended hammerhead crystal structure with the existing biochemical data is a promising sign that this structure represents the active conformation. However, there exists a scarcity of experiments designed specifically to test the newly proposed catalytic mechanism. Such an investigation is especially timely in light of past hammerhead ribozyme structures, some of which have not been entirely consistent with biochemical studies. Thus, we have developed a new affinity labeling technique to probe ribozyme activity,<sup>28</sup> and herein, we apply this mechanistic probe to the hammerhead ribozyme in order to provide fresh insight into the catalytic mechanism.

The affinity labeling approach to identify the general base in enzyme catalyzed ribophosphodiester cleavage was first applied to RNaseA,<sup>29</sup> which confirmed the identity of His12 as the general base in that case. The 2'-OH at the scissile ribose, which must normally be deprotonated during substrate cleavage, is replaced by a 2'-bromoacetamide group. This reactive electrophile is poised to alkylate, and tag for identification, a ribozyme residue responsible for general base catalysis (Scheme 2). We have recently applied this experiment to a ribozyme for the first time with the hairpin ribozyme, and now extend this methodology to the hammerhead ribozyme.

The data presented herein convincingly suggest that the deprotonated N1 of G12 is directly responsible for general base catalysis in the hammerhead ribozyme. Alkylation of several other ribozyme residues, which do not appear to be involved in general base catalysis, suggests the existence of a population of inactive ribozyme conformation(s). This study also provides important context for our recent hairpin ribozyme experiments; some significant differences of possible mechanistic implication are highlighted and discussed. Finally, this study also demonstrates the generality of the 2'-bromoacetamide affinity labeling approach in probing RNA-cleaving catalysts and shows how privileged active site structures in ribozymes can be readily revealed by chemical probing techniques.

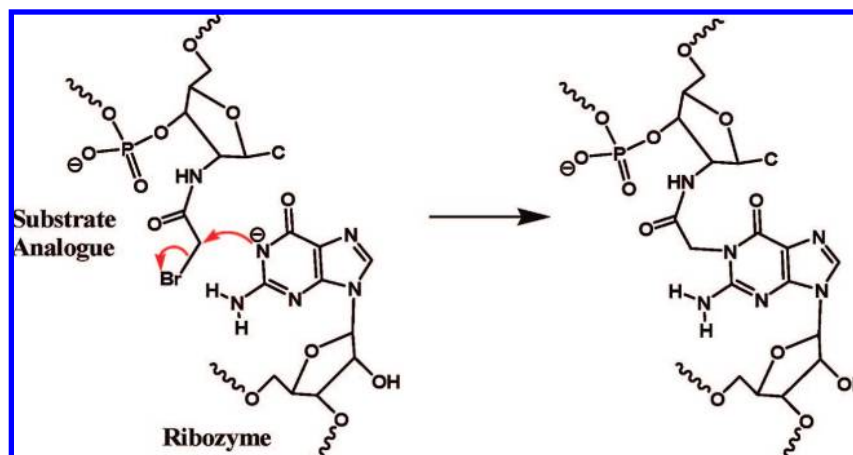
## Materials and Methods

**Chemicals and Biochemicals.** All chemicals and buffers salts were purchased from Sigma-Aldrich. DNA and RNA oligonucleotides were synthesized by the University of Calgary DNA Services Laboratory. RNA was also synthesized by in vitro transcription from synthetic DNA templates using the T7 Mega Short Script kit (Ambion).  $\gamma$ -<sup>32</sup>P-ATP and 5'-<sup>32</sup>P-pCp were purchased from Perkin-Elmer. T4 polynucleotide kinase and terminal transferase were purchased from Invitrogen, RNase A, RNase T1, and shrimp

- (14) Pley, H. W.; Flaherty, K. M.; McKay, D. B. *Nature* **1994**, *372*, 68–74.  
 (15) Nowakowski, J.; Shim, P. J.; Prasad, G. S.; Stout, C. D.; Joyce, G. F. *Nat. Struct. Biol.* **1999**, *6*, 151–156.  
 (16) Khvorova, A.; Lescoute, A.; Westhof, E.; Jayasena, S. D. *Nat. Struct. Biol.* **2003**, *10*, 708–712.  
 (17) Canny, M. D.; Jucker, F. M.; Kellogg, E.; Khvorova, A.; Jayasena, S. D.; Pardi, A. *J. Am. Chem. Soc.* **2004**, *126*, 10848–10849.  
 (18) Heckman, J. E.; Lambert, D.; Burke, J. M. *Biochemistry* **2005**, *44*, 4148–4156.  
 (19) Lambert, D.; Heckman, J. E.; Burke, J. M. *Biochemistry* **2006**, *45*, 7140–7147.  
 (20) Han, J.; Burke, J. M. *Biochemistry* **2005**, *44*, 7864–7870.  
 (21) Martick, M.; Scott, W. G. *Cell* **2006**, *126*, 309–320.  
 (22) Lee, T.-S.; Silva-Lopez, C.; Martick, M.; Scott, W. G.; York, D. M. *J. Chem. Theory Comput.* **2007**, *3*, 325–327.  
 (23) Martick, M.; Lee, T.-S.; York, D. M.; Scott, W. G. *Chem. Biol.* **2008**, *15*, 332–342.  
 (24) Chi, Y.-I.; Martick, M.; Lares, M.; Kim, R.; Scott, W. G.; Kim, S.-H. *PLoS Biol.* **2008**, *6*, e234.

- (25) Lee, T.-S.; Lopez, C. S.; Giambasu, G. M.; Martick, M.; Scott, W. G.; York, D. M. *J. Am. Chem. Soc.* **2008**, *130*, 3053–3064.  
 (26) Lee, T.-S.; York, D. M. *J. Am. Chem. Soc.* **2008**, *130*, 7168–7169.  
 (27) Roychowdhury-Saha, M.; Burke, D. H. *RNA* **2006**, *12*, 1846–1852.  
 (28) Thomas, J. M.; Perrin, D. M. *J. Am. Chem. Soc.* **2006**, *128*, 16540–16545.  
 (29) Hummel, C. F.; Pincus, M. R.; Brandt-Rauf, P. W.; Frei, G. M.; Carty, R. P. *Biochemistry* **1987**, *26*, 135–146.

Scheme 2. Alkylation of a Deprotonated Guanosine-N1 by the 2-Bromoacetamide Probe



alkaline phosphatase from Fermentas, RNA ligase from New England Biolabs, and Superase-in RNase inhibitor from Ambion. The *N*-hydroxy-succinimidyl ester of bromoacetate was freshly prepared every week, as previously described,<sup>30</sup> and stored at  $-20^{\circ}\text{C}$  under argon.

**Oligonucleotide Sequences.** The trans-cleaving *S. mansoni* ribozyme and substrate sequence were taken from Canny et al.<sup>17</sup> WT ribozyme sequence: 5'-GGCGAGGUACAUCACGACGAGUC-CCAAAUAGGACGAAAUGCCC-3' (mutations made to this sequence are described in the text and figures); 2'-NH<sub>2</sub> substrate analogue: 5'-d(GGGCAT-X-CTGGATTCCACTCGCC) where X is 2'-amino-2'-deoxy-cytidine. The trans-cleaving HH16 ribozyme sequences were taken from Hertel et al.<sup>31</sup>

**Oligonucleotide Preparation.** Hammerhead ribozymes containing only canonical RNA nucleotides were prepared by in vitro transcription from synthetic DNA templates bearing a T7 promoter.<sup>32</sup> In cases where a single noncanonical substitution was incorporated, and for 3'-labeled footprinting experiments, ribozymes were synthesized by standard solid phase phosphoramidite chemistry. Oligonucleotides bearing N7-deaza purine modifications required the use of *t*-butyl-hydroperoxide in the oxidation cycles instead of iodine.<sup>33</sup> All ribozymes were purified by 10% denaturing 7 M urea/TBE PAGE ("d-PAGE"), eluted with 1% LiClO<sub>4</sub>/10 mM Tris-HCl (pH 8) for 30 min at 65 °C, concentrated, ethanol precipitated, and G-25 desalted prior to use. Substrate analogue oligos were purified similarly by 20% d-PAGE.

**Alkylation Reactions.** The 2'-bromoacetamido-substrate analogue was prepared by reacting the 2'-NH<sub>2</sub> substrate analogue with *N*-hydroxysuccinimidyl ester of bromoacetate in DMF/Na-borate buffer (pH 8) as previously described.<sup>28</sup> Alkylation reactions were generally performed in 50 mM MgCl<sub>2</sub>, 100 mM NaCl, and 50 mM buffer (Na-PIPES pH 6.5 and 7, Tris-HCl pH 7.5–8.5, Na-borate pH 9). Variation of metal salts is described in the figures and text. The ribozyme concentration was 2.5 μM (including a trace of 5'-<sup>32</sup>P-labeled ribozyme) and the substrate analogue concentration was 3 μM. Reaction time points were quenched with 3–5 volumes of 90% formamide/50 mM EDTA/0.01% xylene cyanol/0.01% bromophenol blue. Reaction products were resolved by 10% d-PAGE and quantified by phosphorimager (Molecular Dynamics Imagerquant v5.2). In order to minimize the (pH-dependent) effects of bromoacetamide solvolysis over long reaction times needed to complete the alkylation reactions (up to ~50 h), initial rates were

analyzed using early time points (<10–15% of reaction completed). Rate constants (hr<sup>-1</sup>) were determined by linear regression using Sigma Plot. The [Mg<sup>2+</sup>] dependence of G12 alkylation (Figure 7) was fit to the Hill-type binding equation:

$$k_{\text{obs}} = \frac{k_{\text{max}} [\text{Mg}^{2+}]^n}{K_D + [\text{Mg}^{2+}]^n} + k_0 \quad (1)$$

where  $k_{\text{max}}$  is the rate constant at saturating [Mg<sup>2+</sup>],  $k_0$  is the rate constant at [Mg<sup>2+</sup>] = 0,  $n$  is the Hill-type coefficient, and  $K_D$  is the apparent dissociation constant for Mg<sup>2+</sup> binding. The concentration of Mg<sup>2+</sup> required for half-maximal alkylation rate is defined as [Mg<sup>2+</sup>]<sub>1/2</sub> =  $K_D^{(1/n)}$ .

**Alkylation Site Footprinting.** For experiments with 5'-labeled ribozyme, the 2'-NH<sub>2</sub> substrate analogue was 5'-phosphorylated using unlabeled ATP and T4 polynucleotide kinase prior to bromoacetylation. Ribozyme transcripts were dephosphorylated by treatment with shrimp alkaline phosphatase. Phosphatase was heat inactivated at 65° for 10 min. The samples were extracted twice with phenol/chloroform, ethanol precipitated, and desalted over a G-25 spin column. Alkylation reactions were carried out as described above at pH 7.5, but on a larger scale (~1–2 nmol ribozyme). The reactions were quenched after 48 h by addition of a stoichiometric quantity of EDTA with respect to the Mg<sup>2+</sup> in the sample. The samples were then butanol concentrated and ethanol precipitated. Unlabeled ribozyme alkylation products were resolved by 10% d-PAGE and desalted as described above for the ribozymes. The purified alkylated ribozyme was then 5'-radiolabeled using γ-<sup>32</sup>P-ATP and T4 polynucleotide kinase. Only the 5'-end of the ribozyme is radiolabeled, as the 5'-end of the substrate analogue was blocked by prior phosphorylation.

For experiments with 3'-labeled ribozyme, the 3'-end of the 2'-NH<sub>2</sub> substrate analogue was extended with 2',3'-dideoxy-ATP and terminal transferase prior to bromoacetylation. Alkylation reactions were performed and the products purified as described for the 5'-labeled samples above. Only synthetic ribozymes were used as 3'-sequence inhomogeneity in runoff transcripts proved detrimental to footprinting experiments. The purified, alkylated ribozyme was then 3'-radiolabeled using <sup>32</sup>P-pCp and RNA ligase. Only the 3'-end of ribozyme is radiolabeled, as the reaction is blocked for the substrate analogue by its 3'-dideoxy terminus.

Following radiolabeling, both the 5'- and 3'-labeled samples were repurified by 10% d-PAGE and desalted before footprinting analysis. To generate the alkaline hydrolysis ladders, samples were treated with 0.5% K<sub>2</sub>CO<sub>3</sub> (pH 10.3 at 22 °C) at 95 °C for 4 min. To generate the G-specific cleavage ladders, samples were combined with 5 nmol of carrier RNA (unlabeled ribozyme) in 10 μL of 10 mM Tris-HCl (pH 7.5) and treated with 1 unit of RNase T1 at 37 °C for 4 min. Reactions were terminated by adding 2 volumes of

(30) Povsic, T. J.; Dervan, P. B. *J. Am. Chem. Soc.* **1990**, *112*, 9428–9430.

(31) Hertel, K. J.; Herschlag, D. J. A.; Uhlenbeck, O. C. *Biochemistry* **1994**, *33*, 3374–3385.

(32) Milligan, J. F.; Groebe, D. R.; Witherell, G. W.; Uhlenbeck, O. C. *Nucleic Acids Res.* **1987**, *15*, 8783–8798.

(33) Sproat, B.; Colonna, F.; Mullah, B.; Tsou, D.; Andrus, A.; Hampel, A.; Vinayak, R. *Nucl. and Nucl.* **1995**, *14*, 255–273.

90% formamide/50 mM EDTA/0.01% xylene cyanol/0.01% bromophenol blue and placing the samples on ice. The digestions were immediately analyzed on 10% or 12% d-PAGE sequencing gels as indicated in figure legends. A secondary structure compression interfered with routine d-PAGE analysis of the 3'-labeled samples; it was necessary to run these gels at higher temperature by applying power of 100 W instead of the standard 40 W.

**Aniline Footprinting.** 3'-Labeled alkylated ribozyme samples were treated with 0.5 M anilinium-acetate (pH 4.5) at 37 °C for 20 min in 10  $\mu$ L. The samples were then lyophilized, and twice resuspended in 50  $\mu$ L water and re-lyophilized. Alkaline and RNase T1 digestions were performed as above with the exception that the reactions were not stopped by addition of formamide/EDTA. The alkaline digestions were stopped by chilling on ice and neutralizing with 10 mM HCl, whereas the RNase T1 digestions were stopped by adding 5 units RNase inhibitor (Ambion). In order to harmonize the phosphorylation states of the digestion products resulting from all of alkaline, RNase T1, and aniline treatments, all samples were subsequently treated with polynucleotide kinase and unlabeled ATP (1 mM). Digestion samples were diluted into 10 volumes of polynucleotide kinase buffer and treated with 20 units of the enzyme for 2 h at 37 °C. Samples were analyzed by 12% d-PAGE sequencing gels run at 100 W.

## Results

The general base alkylation experiment for the hammerhead ribozyme was performed in direct analogy to our previous experiment with the hairpin ribozyme.<sup>28</sup> Specifically, a substrate analogue bearing an electrophilic 2'-bromoacetamide in place of the cleavage site 2'-OH was reacted in trans with the hammerhead ribozyme. The standard reaction conditions were 2.5  $\mu$ M ribozyme, 3  $\mu$ M substrate analogue, 50 mM MgCl<sub>2</sub>, 100 mM NaCl, and 50 mM Tris-HCl (pH 8) at room temperature in the dark. Initially, the experiment was attempted using a trans-acting HH16 minimal hammerhead ribozyme, but yields of alkylated ribozyme were low, and the separation and analysis of what appeared to be two or more alkylation products proved to be intractable (Figure 2).

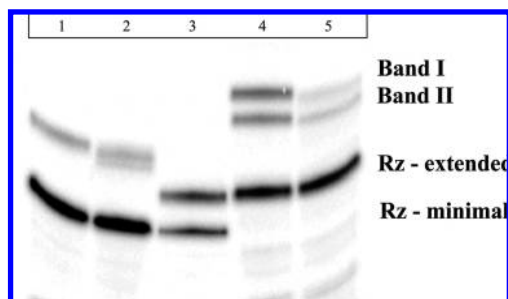


**Figure 2.** Alkylation of the HH16 (minimal) and the *S. mansoni* (extended) hammerhead ribozymes (5'-<sup>32</sup>P labeled) with ribo- and deoxyribo-bromoacetamide substrate analogues in 50 mM MgCl<sub>2</sub>, 100 mM NaCl, and 50 mM Tris-HCl pH 7.5 for 24 h. The alkylation bands characterized in this study (I and II) are indicated. Lane 1: HH16 ribozyme + deoxy-substrate analogue. Lane 2: HH16 ribozyme + ribo-substrate analogue. Lane 3: Cospot of unreacted HH16 and *S. mansoni* ribozymes. Lane 4: *S. mansoni* + deoxy-substrate analogue. Lane 5: *S. mansoni* + ribo-substrate analogue. Samples were analyzed by 10% d-PAGE. Rz = ribozyme.

In keeping with the trend of increased cleavage activity from minimal to extended hammerheads,<sup>16,17</sup> the alkylation reaction was more fruitful for the trans-acting *S. mansoni* extended hammerhead than for the HH16 minimal hammerhead. The two alkylation products (bands I and II) observed for the *S. mansoni* ribozyme appeared in greater yield and were much better resolved by PAGE than those of the HH16 ribozyme (Figure 2).

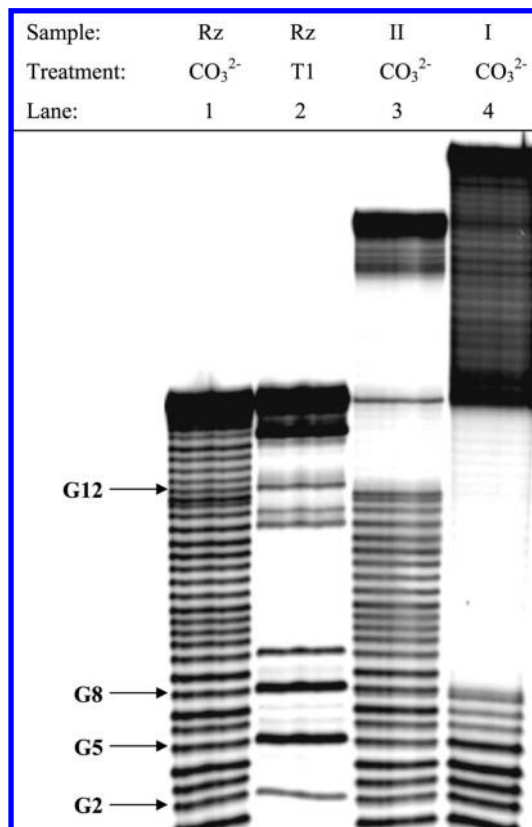


**Figure 3.** Alkaline footprinting of wildtype 5'-<sup>32</sup>P-labeled ribozyme alkylation products. Lane 1: ribozyme treated with 0.5% K<sub>2</sub>CO<sub>3</sub> at 95 °C for 5 min. Lane 2: ribozyme treated with RNase T1. Lane 3: band II treated with 0.5% K<sub>2</sub>CO<sub>3</sub> at 95 °C for 5 min. Lane 4: band I treated with 0.5% K<sub>2</sub>CO<sub>3</sub> at 95 °C for 5 min. Samples were analyzed by 10% d-PAGE.

Using footprinting analysis, we sought to determine the sites of ribozyme alkylation for both bands. Thus, bands I and II were excised and radiolabeled specifically at the 5'-end of the ribozyme strand and repurified by d-PAGE. The alkylation products resulting from the reaction of an all-RNA substrate analogue proved to be refractory to clear alkaline footprint analysis (data not shown). Given that DNA substrates with a single embedded ribose at the cleavage site are efficiently cleaved by both minimal<sup>34</sup> and extended<sup>35</sup> hammerheads, we simplified this analysis by using a DNA substrate analogue, with a single embedded 2'-bromoacetamido-C at the native cleavage site. Not only were the yields of bands I and II unexpectedly enhanced (Figure 2), but both bands produced much clearer alkaline footprint patterns because only the labeled ribozyme strand is susceptible to alkaline cleavage.

The alkylated residue on the 5'-labeled ribozyme is identified from the alkaline footprinting pattern by the first cleavage band with drastically increased molecular weight due to covalent linkage to the substrate analogue strand.<sup>36</sup> Footprinting analysis in Figure 3 (lane 3) clearly identifies G12 as the site of ribozyme alkylation for band II based on comparison to the RNase T1 (G specific) sequencing ladder (lane 2). In contrast to band II, the footprinting pattern for band I (lane 4) appears more complex. Clearly, the band corresponding to cleavage at A9 is

(34) Yang, J.-H.; Perreault, J. P.; Labuda, D.; Usman, N.; Cedergren, R. *Biochemistry* **1990**, *29*, 11156–11160.

(35) Unpublished results.

(36) For a pictorial explanation of alkaline footprint interpretation for the 5'- and 3'-labeled samples, see Supporting Information.

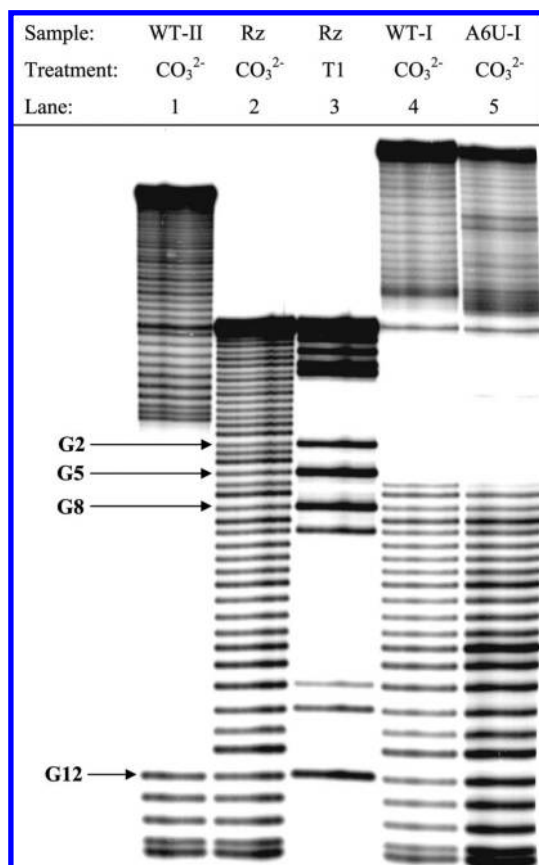


**Figure 4.** Alkaline footprinting of wildtype and mutant 3'-<sup>32</sup>P-labeled ribozyme alkylation products. K<sub>2</sub>CO<sub>3</sub> and RNase T1 treatments were as described for Figure 3. Samples were analyzed by 12% d-PAGE.

completely shifted, indicating alkylation at A9; however, the cleavage band intensity also drops markedly at A6 relative to the more uniform band intensities observed for alkaline cleavage of the ribozyme (lane 1). This suggests that band I represents a mixture of alkylations of both A6 and A9. Indeed, mutation of A6 to U, restored the uniform band intensity up to the completely shifted A9 band (see Supporting Information), demonstrating that the anomalous intensity pattern for the wildtype sample was the result of A6 alkylation. In addition, an unidentified cleavage band that is inconsistent with the normal carbonate-induced cleavage bands also appears between C7 and G8 in the band I footprint. More detailed examination of this species suggested that this band represents cleavage at an abasic site that first formed as a result alkylation-induced depurination (see Supporting Information).

In order to confirm that band II represents alkylation of G12 alone, and to further investigate the nature of band I, we footprinted the same bands I and II after they were labeled at the 3'-end of the ribozyme (Figure 4). By doing this, the site of ribozyme alkylation is identified in the alkaline footprint by the last unshifted cleavage band.<sup>36</sup> In agreement with the 5'-footprinting data, the band II alkaline footprint (lane 1) clearly shows a shift in molecular weight after G12, which confirms that band II represents a pure sample, alkylated only at G12. The alkaline footprint of band I (lane 4) clearly shifts after A6, thus confirming that band I represents a mixture of A6, A9, but possibly other alkylation linkages in the intervening sequence (C7 or G8). In agreement with the 5'-labeled footprint, the A6U substitution drastically reduces alkylation of this residue; the

resulting footprinting pattern indicates alkylation of C7, at least for the A6U mutant (Figure 4, lane 5).

To probe for alkylation lesions at C7 and G8 in the wildtype ribozyme, which would not be readily identified in the above alkaline footprinting experiments, the 3'-labeled samples were treated with anilinium-acetate (pH 4.5). This treatment reveals, by strand cleavage, any abasic sites which would result from depurination/depyrimidination of alkylated residues.<sup>37</sup> Aniline-catalyzed strand cleavage proceeds via  $\beta$ -elimination to afford 3'-<sup>32</sup>P-labeled fragments bearing 5'-phosphorylated termini, which exhibit altered d-PAGE mobility when compared to the 5'-OH terminated fragments generated by RNase T1 or alkaline cleavage. In order to facilitate direct comparison with the alkaline footprint and RNase T1 sequencing patterns, all samples were treated with polynucleotide kinase and ATP to synchronize the 3'- and 5'-phosphorylation states.<sup>38</sup> Aniline treatment of band I (Figure 5A, Lane 6) revealed cleavage at A6, C7, G8, and A9, suggesting that band I consists of a mixture of ribozymes alkylated at any one of these positions. Quantification of the components of the mixture based on this data is problematic due to variation of the rate of abasic site formation with nucleobase and alkylation site. Mutation of A6 and C7 to U, as well as mutation of A9 to 7-deaza-A diminished aniline cleavage at these residues which provides confirmation of the sequence assignment of the aniline cleavage sites (Figure 5B).

We then attempted to ascertain which atom had been alkylated on each of G8, A9, and G12, as these residues were present in the active site observed in the *S. mansoni* crystal structure. To this end, we first tested whether the N7 atom of these purines had been alkylated. The N7 position of guanine is generally among the most nucleophilic positions in nucleic acids,<sup>39,40</sup> but is a very weak base;<sup>41</sup> therefore, N7 alkylation is not likely to reflect general base activity, but rather fortuitous positioning of the nucleophile near the bromoacetamide electrophile. G12 alkylation rate was not significantly affected in the 7-deaza-G12 mutant ("G12c<sup>7</sup>") demonstrating that N7 of G12 is not alkylated (Table 1); moreover, band II is not significantly affected by aniline treatment (Figure 5A, lane 1), suggesting that alkylation occurred at N1 (N7 or N3 alkylations accelerate depurination, whereas N1 alkylation does not).<sup>42</sup> The 7-deaza-A9 substitution ("A9c<sup>7</sup>") nearly eliminated aniline cleavage at A9 (Figure 5B, lane5), suggesting that the N7 atom of A9 is alkylated. The 7-deaza-G8 substitution ("G8c<sup>7</sup>") had little effect on the rate of band I appearance or on the strong aniline cleavage at G8 (Figure 5B, lane 4). These observations suggest alkylation occurs at N3 of G8 (N1 alkylation is not suspected as this should not lead to significant depurination and subsequent aniline cleavage<sup>42</sup>).

Next, we sought to compare the properties of the alkylation reaction with those of the catalytic reaction in an effort to gauge whether one or both of the G12 or A6-A9 alkylation events

(37) Nishikawa, K.; Adams, B. L.; Hecht, S. M. *J. Am. Chem. Soc.* **1982**, *104*, 328–330.

(38) Polynucleotide kinase treatment ensures the 5'-phosphorylation and 3'-dephosphorylation of all fragments. See Supporting Information for a comparison of base versus aniline catalyzed cleavage mechanisms and products.

(39) Singer, B. *Biochemistry* **1972**, *11*, 3939–3947.

(40) Jones, J. W.; Robins, R. K. *J. Am. Chem. Soc.* **1963**, *85*, 193–201.

(41) Saenger, W. *Principles of Nucleic Acid Structure*; Springer-Verlag: New York, 1984.

(42) Selzer, R. R.; Elfarra, A. A. *Chem. Res. Toxicol.* **1996**, *9*, 126–132.

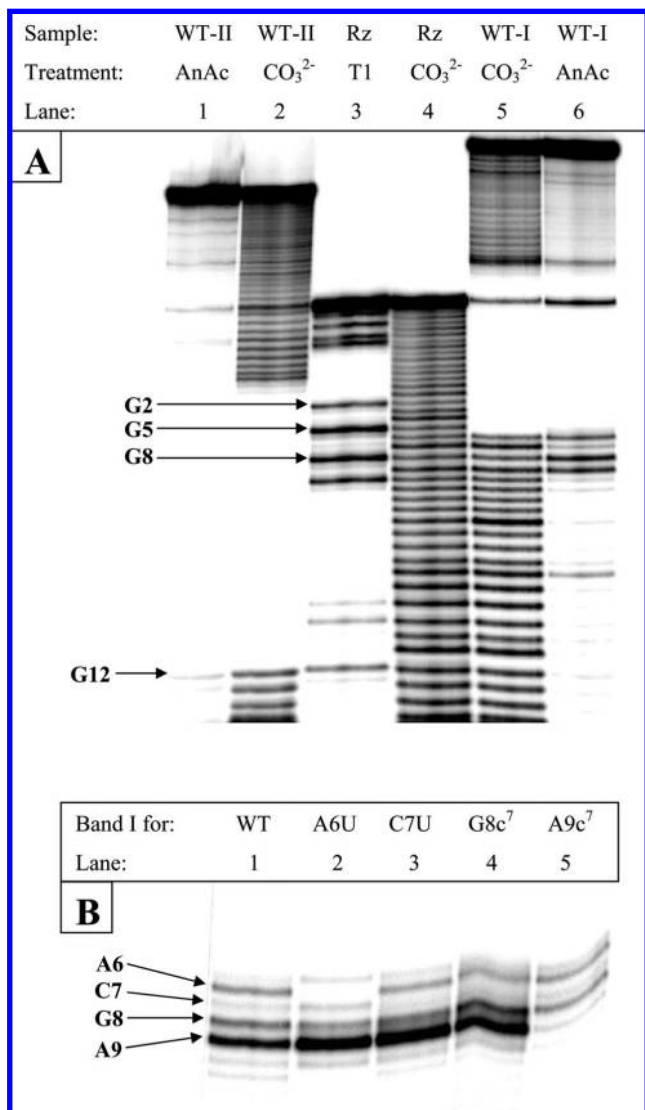


**Figure 5.** (A) Comparison of aniline and alkaline footprints for bands I and II (<sup>32</sup>P-labeled wildtype ribozyme). Lane 1: band I treated with AnAc (0.5 M aniline-acetate pH 4.5) for 20 min. at 37 °C. Lane 2: band I treated with K<sub>2</sub>CO<sub>3</sub> as in Figure 3. Lane 3: Ribozyme treated with RNase T1. Lane 4: Ribozyme treated with K<sub>2</sub>CO<sub>3</sub>. Lane 5: band II treated with K<sub>2</sub>CO<sub>3</sub>. Lane 6: band II treated with AnAc as above. To facilitate direct comparison of electrophoretic mobilities, all samples were treated with polynucleotide kinase and ATP to synchronize the 3'- and 5'-phosphorylation states before analysis by 12% d-PAGE. (B) Close up view of AnAc footprint (generated as above) of band I for the indicated mutant ribozymes. The wildtype is shown as a migration standard.

reflect the catalytic mechanism (Table 1).<sup>43</sup> The formation of both bands I and II was completely inhibited by the addition of (nonbromoacetylated) 2'-NH<sub>2</sub>-substrate analogue, demonstrating that the alkylation reactions depend upon normal substrate binding to the ribozyme. Various residues in the vicinity of the active site observed in the *S. mansoni* crystal structure were mutated and the effects on alkylation rates determined (Table 1). Two mutations had notable effect: A14G significantly diminished, whereas G12A enhanced the formation of band II (G12 alkylation); both had little effect on band I formation (Figure 6 and Table 1). All other mutations had only modest

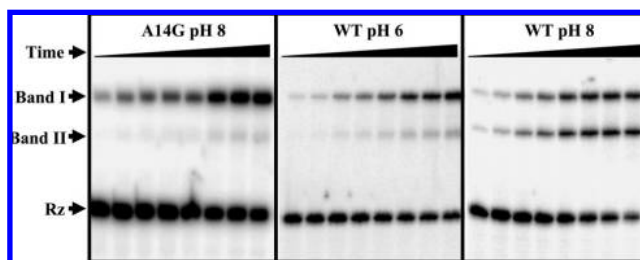
(43) Initial rates were quantified in order to avoid complications due to hydrolysis of the bromoacetamide-substrate analogue at longer time points required to observe completion of the alkylation reaction.

**Table 1.** Rate Constants for the Formation of Bands I and II for the Wildtype Ribozyme under Various Conditions in 50 mM Tris-HCl pH 8, and for Various Mutant Ribozymes in 50mM MgCl<sub>2</sub>, 100 mM NaCl, 50 mM Tris-HCl pH 8. (n.d. = not detected)

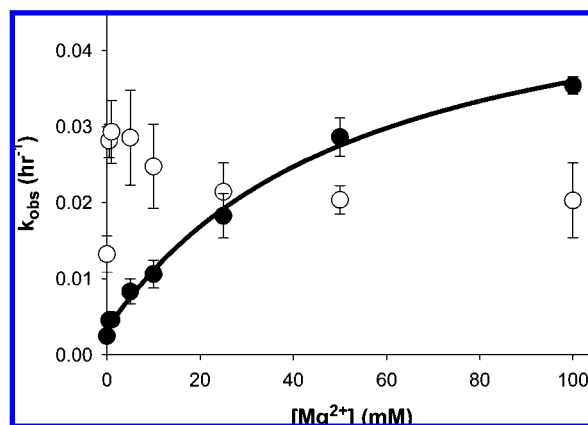
conditions (WT)	band I: $k_{\text{obs}}$ (hr) <sup>-1</sup>	band II: $k_{\text{obs}}$ (hr) <sup>-1</sup>
50 mM MgCl <sub>2</sub> , 100 mM NaCl	0.020	0.021
10 μM 2'-NH <sub>2</sub>	n.d.	n.d.
100 mM NaCl	0.013	0.0025
50 mM Co(NH <sub>3</sub> ) <sub>6</sub> Cl <sub>3</sub>	0.032	0.009

ribozyme	band I: $k_{\text{obs}}$ (hr) <sup>-1</sup>	band II: $k_{\text{obs}}$ (hr) <sup>-1</sup>
WT	0.020	0.021
A14G	0.035	0.0017
G12A	0.018	0.073
G12c <sup>7</sup>	0.022	0.015
A9U	0.0070	0.030
A9c <sup>7</sup>	0.017	0.024
G8c <sup>7</sup>	0.014	0.013
dG8	0.015	0.017
G8A	0.017	0.010
A6U	0.0091	0.0068



**Figure 6.** Alkylation reaction time courses for the 5'-<sup>32</sup>P-labeled wild type and A14G mutant ribozymes in 50 mM buffer (at the indicated pH), 100 mM NaCl, 50 mM MgCl<sub>2</sub>. The same time points were taken to 48 h in each case. Bands I and II, and unreacted 5'-labeled ribozyme (Rz) were resolved by 10% d-PAGE.



**Figure 7.** [Mg<sup>2+</sup>] dependence of the rate constants for (O) band I and (●) band II formation. The 0 mM Mg<sup>2+</sup> reaction contained 5 mM EDTA, and all reactions contained 100 mM NaCl and 50 mM Tris-HCl pH 8.2. The data for band II (G12 alkylation) were fit to eq 1 yielding  $k_{\text{max}} = 0.049$  h<sup>-1</sup>, [Mg<sup>2+</sup>]<sub>1/2</sub> = 47 mM, and a Hill-type coefficient  $n = 1.05$ .

effects on alkylation, contrary to the substantial inhibition (orders of magnitude) of native catalysis observed for all of these mutations.<sup>2,35</sup>

The influence of metal cations on the alkylation reaction was also investigated. The [Mg<sup>2+</sup>] dependence of band I and II formation is plotted in Figure 7. The data for band II (G12 alkylation) fit quite well ( $R^2 = 0.98$ ) to equation 1 for a two-state Mg<sup>2+</sup> binding model, yielding a [Mg<sup>2+</sup>]<sub>1/2</sub> of 47 mM and

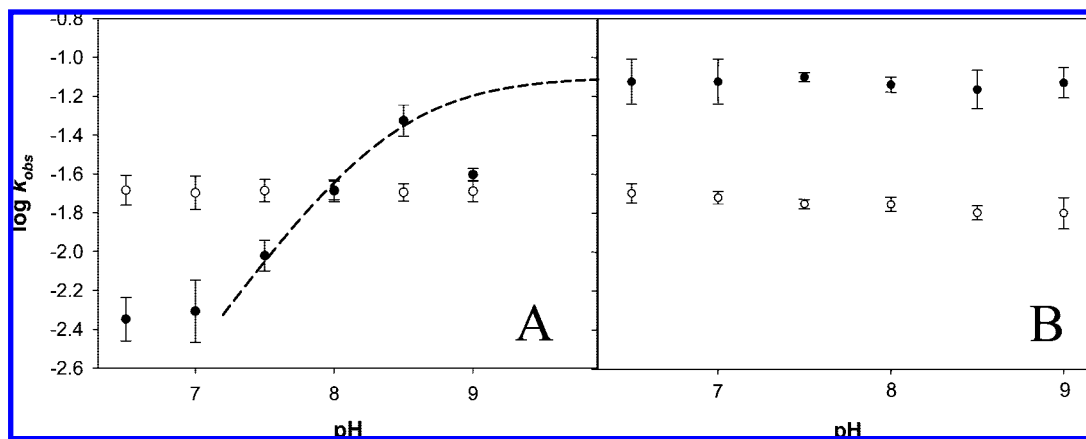


**Figure 8.** pH-rate profiles for alkylation of the (A) wildtype and (B) G12A hammerhead ribozymes in 50 mM buffer, 100 mM NaCl, 50 mM MgCl<sub>2</sub>. The logarithm of the rate constants (hr<sup>-1</sup>) for the formation of (○) band I and (●) band II are plotted as a function of pH. The G12 pH-rate profile (----) is simulated according to  $k_{\text{obs}} = k_{\text{max}}/(1 + 10^{\text{pK}_a - \text{pH}})$ , with  $\log(k_{\text{max}}) = \log(k_{\text{G12A}}) = -1.1$  and  $\text{pK}_a = 8.4$  for N1 of G12.<sup>27</sup>

a Hill-type coefficient,  $n = 1.05$ . Notably, in the absence of Mg<sup>2+</sup> (100 mM NaCl, 5 mM EDTA, 50 mM Tris-HCl, pH 8.2) significant formation of bands I and II is still observed. Under these conditions, the rate constant  $k_{\text{obs}}$  of G12 alkylation is diminished by almost 2 orders of magnitude relative to  $k_{\text{max}}$  at saturating [Mg<sup>2+</sup>], whereas A6–A9 alkylation is only modestly affected. In the presence of 100 mM Co(NH<sub>3</sub>)<sub>6</sub><sup>3+</sup>, the alkylation rates are similar to those in 50 mM Mg<sup>2+</sup>, with the rate of formation of band I elevated slightly and that of band II diminished slightly.

The pH-rate profiles for the formation of bands I and II were investigated for both the wildtype and G12A substituted ribozymes. The rate of G12 alkylation (band II) in the wild type was strongly pH dependent (Figure 6 and 8A). The G12 alkylation rate constant shows a log-linear increase (slope of ~1) from pH 7 to 8.5, as does the rate constant for the native cleavage reaction.<sup>17</sup> When G12 was mutated to A, the pH-dependence of the alkylation rate constant was completely abolished (Figure 8B). Also, the maximum rate of G12 alkylation at pH 8.5, where N1 of G12 is presumably fully deprotonated, approaches the rate of A12 alkylation in the G12A mutant (Figure 8A). These observations appear to reflect the titration of N1 of G12, whereas the G12A mutant presents the fully deprotonated N1 position at all pH's studied; this is illustrated by simulation of the G12 alkylation pH-rate-profile where  $\text{pK}_a = 8.4$  was assumed for N1 of G12,<sup>27</sup> and  $k_{\text{max}}$  was set at the value of  $k_{\text{G12A}}$ . In contrast to the simulation and to the cleavage reaction pH-rate profile, the G12 alkylation rate diminishes abruptly above ~pH 8.5 and is pH-independent upon pH for either of the wildtype or G12A mutant ribozymes (Figures 8, parts A and B), suggesting the alkylations of A6, C7, G8, or A9 occur at a nontitratable positions ( $\text{pK}_a < 7$ ).

## Discussion

The mechanism-based affinity probe method described here was first applied to the protein enzyme RNaseA, where His12 alkylation identified this residue as the general base.<sup>44</sup> We recently extended this experiment to a ribozyme for the first time to probe for possible nucleobase participation in general base catalysis,<sup>28</sup> which had been hypothesized to be operative

in the hairpin ribozyme.<sup>45–47</sup> We have now applied this experiment to the hammerhead ribozyme, where it has been hypothesized, based on the recent crystallography data, that G12 performs general base catalysis.<sup>21</sup> Our current results also provide important context for our previous findings with the hairpin ribozyme, as clear differences have emerged between the two experiments.

In this work, multiple alkylation sites have been identified for the hammerhead ribozyme, whereas the hairpin ribozyme was uniquely alkylated at G8.<sup>28</sup> Alkylation was identified at A6, C7, N3 of G8, N7 of A9, and N1 of G12 in the *S. mansoni* hammerhead. Only alkylation of N1 of G12 and N7 of A9 are structurally consistent with the recent crystallographic data (Figure 9A), in that these positions are in close proximity to the scissile 2'-OH in the active site. In the minimal hammerhead ribozyme crystal structure, (Figure 9B) A6 is close to the scissile 2'-OH, suggesting that alkylation of this residue reflects population of this inactive conformation in the extended hammerhead as well. Neither crystal structure is consistent with alkylation of C7 or G8, suggesting that these reactions represent unobserved folding intermediates, or the trajectory of these residues relative to the cleavage site during the transition from the inactive to the active fold. These results underscore the conformational plasticity of the hammerhead-substrate complex, as opposed to the hairpin ribozyme for which only one fold could be detected by alkylation.<sup>28</sup>

In order to assign a role in general base catalysis to one of the alkylated residues in the hammerhead ribozyme, pH-rate profiles were examined. The sum of the alkylation rates of A6, C7, G8, and A9 (band I) are completely pH-independent (Figure 8, parts A and B). This implies that observation of these alkylations offers only structural insight, reflecting fortuitous alkylation of nontitratable positions which are not likely to be involved in general base catalysis. Conversely, alkylation at G12 in the wild type ribozyme was strongly pH-dependent, mirroring the log-linear increase in native cleavage rate<sup>17</sup> with increasing pH from ~7 to ~8.5 (Figure 8A). The G12A substitution abolished this pH-dependence and further increased alkylation rate (Figure 8B). These effects are consistent with substitution

(45) Bevilacqua, P. C. *Biochemistry* **2003**, *42*, 2259–2265.

(46) Ferré-D'Amaré, A. R. *Biopolymers* **2003**, *73*, 71–78.

(47) Fedor, M. J.; Williamson, J. R. *Nat. Rev. Mol. Cell Biol.* **2005**, *19*, 27–37.

(44) Hummel, C. F.; Pincus, M. R.; Brandt-Rauf, P. W.; Frei, G. M.; Carty, R. P. *Biochemistry* **1987**, *26*, 135–146.

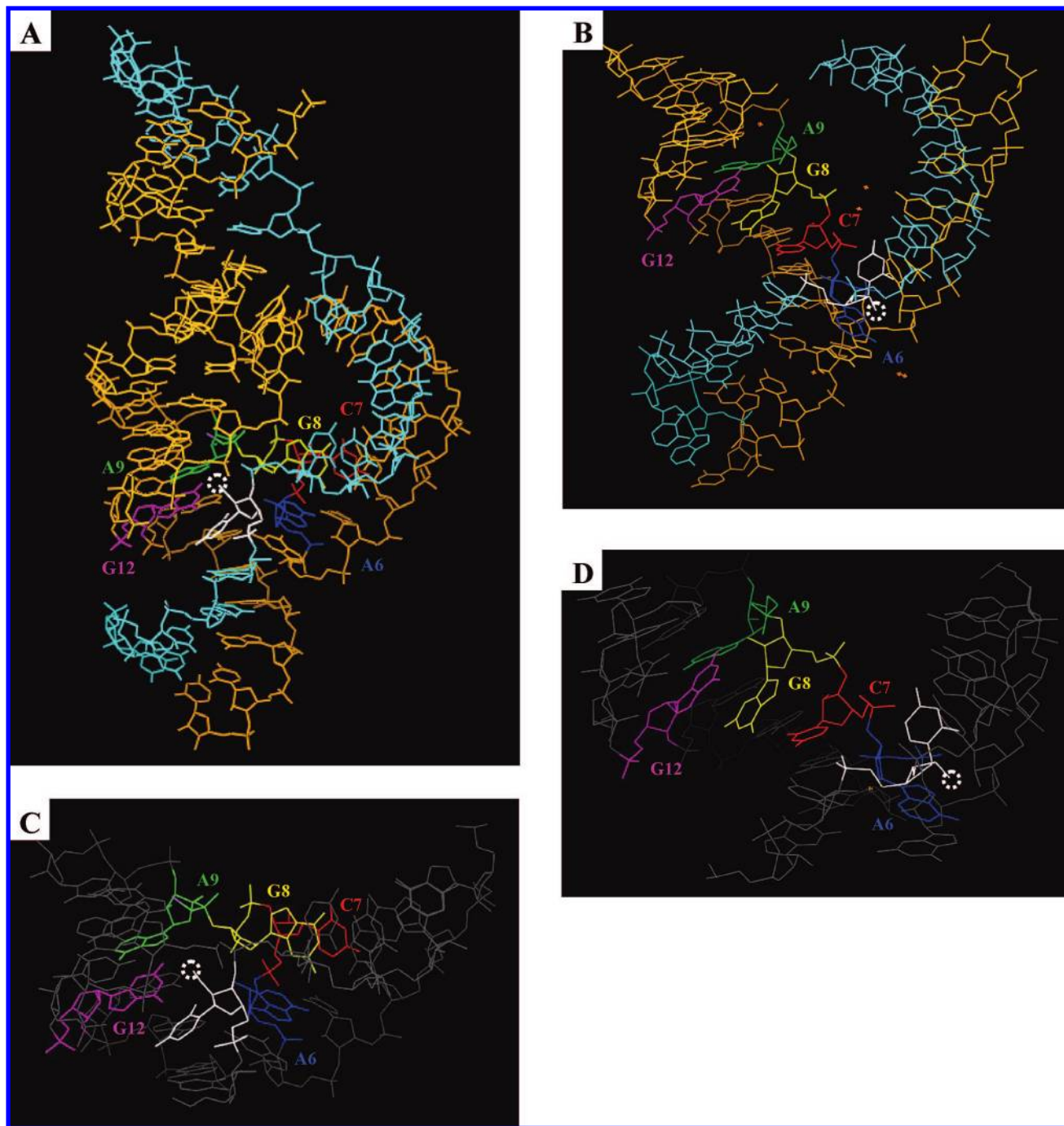


**Figure 9.** Structural images generated using PyMOL from the *S. mansoni* and the minimal hammerhead ribozyme crystal structures.<sup>13,21</sup> The nucleotides identified by affinity labeling in this study are color coded as indicated in the figures. The scissile substrate residues are white, and a dotted white circle indicates the 2'OH/OMe position which was modified with the reactive bromoacetamide. The full crystal structures are depicted for (A) the *S. mansoni* and (B) the minimal hammerheads, with the ribozyme strand in orange and the substrate strand in teal. Close-up images focused on the nucleotides of interest here are presented for (C) the *S. mansoni* and (D) the minimal hammerheads ribozymes.

of the fully deprotonated N1 of A12 ( $pK_a$  of conjugate acid of N1 of adenosine is 3.7<sup>41</sup>), and confirm that the wildtype pH-dependence reflects alkylation of the titratable N1 position of G12. Strikingly, at pH 8.5, where N1 of G12 appears to be largely deprotonated, the rate constant for its alkylation approaches that of the completely deprotonated N1 of the A12 substitution. This is illustrated by the simulation in Figure 8A, which assumes a  $pK_a$  value of 8.4 for N1 of G12<sup>27</sup> and a maximum rate constant equal to that observed for A12 alkylation. These results strongly imply a direct role in general base

catalysis for deprotonated N1 of G12, and suggest that its  $pK_a$  is perturbed downward (the  $pK_a$  of free guanosine-3',5'-bis(ethyl phosphate) is 9.57).<sup>48</sup> The pH-rate profile for wildtype G12 alkylation levels off below pH  $\approx 7$ , contrary to the continued titration of N1 observed for the native cleavage reaction.<sup>17</sup> This effect may stem from a pH-independent alkylation of protonated G12, followed by rapid loss of the N1-proton. The decrease in

(48) Acharya, P.; Acharya, S.; Cheruku, P.; Amirkhanov, N. V.; Földesi, A.; Chattopadhyaya, J. *J. Am. Chem. Soc.* **2003**, *125*, 9948–9961.

G12 alkylation rate at pH 9 is more pronounced than for the native cleavage reaction;<sup>17</sup> it is also curious that this effect is not observed for alkylation of the G12A substitution. This effect does not appear to stem from denaturation at high pH, and may be peculiar to the G12 alkylation reaction and not relevant to catalysis.

The  $[\text{Mg}^{2+}]$  dependence of the G12 alkylation (Figure 7) is very similar to that of the native *S. mansoni* cleavage reaction ( $[\text{Mg}^{2+}]_{1/2} = 40$  mM for cleavage<sup>17</sup> and 47 mM for G12 alkylation, both with a Hill coefficient  $n \approx 1$ ). This further supports the conclusion that G12 alkylation reflects the catalytic mechanism, and supports assignment of the recent crystal structure (Figure 9A) as the active fold.<sup>21</sup> Therefore, the level of G12 alkylation should serve as an indication of the relative population of the active fold (or at least proper placement of G12 in the active site). Although our data confirm that  $\text{Mg}^{2+}$  binding strongly favors the active fold, significant G12 alkylation in the absence of  $\text{Mg}^{2+}$  shows that the active fold is still populated in the presence exchange inert  $\text{Co}(\text{NH}_3)^{3+}$  ions and even in minimal NaCl alone, although to a lesser extent. In contrast, *S. mansoni* hammerhead catalysis is nearly undetectable in 100 mM NaCl, and significantly impaired in 100 mM  $\text{Co}(\text{NH}_3)^{3+}$ .<sup>47</sup> Taken together these data suggest that in the cleavage reaction,  $\text{Mg}^{2+}$  has both a structural role in stabilization of the active fold and a catalytic role other than general base catalysis.

The collective alkylations of A6, C7, G8, and A9 display a  $[\text{Mg}^{2+}]$  dependence completely different from G12 alkylation and the native reaction<sup>17</sup> (Figure 7). At higher  $[\text{Mg}^{2+}]$  ( $>1$  mM), the decrease in A6–A9 alkylation likely partially reflects the depopulation the inactive fold at higher  $[\text{Mg}^{2+}]$  in favor of the active fold. At  $[\text{Mg}^{2+}] < 1$  mM, the rise in A6–A9 alkylation likely reflects the  $\text{Mg}^{2+}$ -assisted formation of the global, Y-shaped fold common to both the active and inactive conformations. Indeed, using FRET, Lilley and co-workers observed  $\text{Mg}^{2+}$ -dependent formation of this global fold; they determined that half the population was folded at  $[\text{Mg}^{2+}] = 160 \mu\text{M}$ ,<sup>48</sup> qualitatively consistent with the behavior of A6–A9 alkylation at  $[\text{Mg}^{2+}] < 1$  mM. Substantial A6–A9 alkylation in NaCl alone also indicates significant formation of the global fold in the absence of  $\text{Mg}^{2+}$ .

The log-linear increase in the rate of G12 alkylation in the hammerhead ribozyme strongly suggests that N1 of G12 functions as a bona fide general base. This result stands in stark contrast to the very weak increase in hairpin ribozyme alkylation at G8 up to pH 9.<sup>28</sup> The basal, pH-independent mechanism observed below pH 7 for hammerhead G12 alkylation appears to dominate in hairpin G8 alkylation, even up to pH 9. This suggests that the hairpin G8 residue has a  $\text{pK}_a > 9$ , at least in the context of the alkylation reaction.<sup>51</sup> This interpretation supports the hypothesis that protonated N1 of G8 stabilizes the hairpin ribozyme transition state by donating a hydrogen bond to stabilize the developing negative charge on the 2'-oxygen via an oxyanion hole-type interaction.<sup>47,52,53</sup> Recent computational results also support this mechanistic hypothesis and suggest that the proton from the nucleophilic 2'-oxygen is accepted by a nonbridging oxygen on the scissile phosphate.<sup>54</sup> Overall, the hammerhead G12 and hairpin G8 residues appear

to stabilize the transition states via two distinct mechanisms, despite their similar structural positioning with their N1 positions juxtaposed to the scissile 2'-OH.

In summary, we have demonstrated pH- and  $[\text{Mg}^{2+}]$ -dependent affinity labeling of the anionic N1 position of G12 in a hammerhead ribozyme. Previous biochemical results suggested a role for G12 in general acid or base catalysis,<sup>20</sup> but ambiguity inherent in the interpretation of cleavage pH-rate profiles prevents the discrimination of these possibilities.<sup>45</sup> Although our results pertain to a different chemical reaction than the native RNA cleavage reaction, they do not suffer from the same kinetic ambiguity, and thus strongly support the newly proposed role for G12 in general base catalysis (Scheme 1).<sup>21–23</sup> The analogous alkylation of His12, the general base in RNaseA,<sup>44</sup> supports this interpretation and underscores the mechanistic parallels shared by ribozymes and protein enzymes. Despite the apparent lack of useful chemical functionality in RNA, compared to wide variety enjoyed by proteins, ribozymes are able to assemble active site structures capable of delivering general acid/base catalysis without the direct involvement of metal ions.<sup>55–61</sup>

**Acknowledgment.** We gratefully acknowledge Prof. George A. Mackie for sharing his expertise in identifying and overcoming secondary structure compression in footprinting gels. This work was funded by NSERC and CIHR. Salary support was provided in the form of NSERC CGS-D and Gladys Estella Laird fellowships (J.M.T.), and a Michael Smith Foundation Senior Career Award (D.M.P.).

**Supporting Information Available:** This material is available free of charge via the Internet at <http://pubs.acs.org>.

JA804496Z

- (51) An important caveat must be entertained: the affinity label may perturb the hairpin ribozyme active site structure such that apparent  $\text{pK}_a$  of G8 is increased relative to its  $\text{pK}_a$  in the presence of native substrate. Moreover, the 2'-bromoacetamide substrate analogue is not, by definition, a mechanism based inhibitor in that its reactivity is not unmasked as a result of the catalytic mechanism. The positioning of the reactive electrophile where substrate deprotonation normally occurs encourages a mechanistic interpretation for ribozyme alkylation, especially where the alkylation rate shows log-linear increase with pH, as for hammerhead G12 alkylation. Caution must be exercised, however, as the high reactivity of the probe may lead to alkylations that reflect only fortuitous structural positioning, not the involvement of a particular residue in general base catalysis. This is exemplified by the apparently pH-independent alkylations of A6, C7, G8, and A9 in the hammerhead, which are not likely to be indicative of general base catalysis.
- (52) Kuzmin, Y. I.; Da Costa, C. P.; Fedor, M. J. *J. Mol. Biol.* **2004**, *340*, 233–251.
- (53) Pinard, R.; Hampel, K. J.; Heckman, J. E.; Lambert, D.; Chan, P. A.; Major, F.; Burke, J. M. *EMBO J.* **2001**, *20*, 6434–6442.
- (54) Nam, K.; Gao, J.; York, D. M. *J. Am. Chem. Soc.* **2007**, *130*, 4680–4691.
- (55) Bevilacqua, P. C.; Yajima, R. *Curr. Opin. Chem. Biol.* **2006**, *10*, 455–464.
- (56) Nakano, S.-I.; Chadalavada, D. M.; Bevilacqua, P. C. *Science* **2000**, *287*, 1493–1497.
- (57) Perrotta, A. T.; Shih, I.; Been, M. D. *Science* **1999**, *286*, 123–126.
- (58) Das, S. R.; Piccirilli, J. A. *Nat. Chem. Biol.* **2005**, *1*, 45–52.
- (59) Zhao, Z. Y.; McLeod, A.; Harusawa, S.; Araki, L.; Yamaguchi, M.; Kurihara, T.; Lilley, D. M. *J. Am. Chem. Soc.* **2005**, *127*, 5026–5027.
- (60) Wilson, T. J.; Ouellet, J.; Zhao, Z. Y.; Harusawa, S.; Araki, L.; Kurihara, T.; Lilley, D. M. *J. RNA* **2006**, *12*, 980–987.
- (61) Kuzmin, Y. I.; Da Costa, C. P.; Cottrell, J. W.; Fedor, M. J. *J. Mol. Biol.* **2005**, *349*, 989–1010.

(49) Manuscript in preparation.

(50) Penedo, J. C.; Wilson, T. J.; Jayasena, S. D.; Khvorova, A.; Lilley, D. M. *RNA* **2004**, *10*, 880–888.